Manuscript published:

Szczypiński, P. M., & Zapotoczny, P. (2012).
Computer vision algorithm for barley kernel identification, orientation estimation and surface structure assessment.
Computers and Electronics in Agriculture, 87, 32-38

http://dx.doi.org/10.1016/j.compag.2012.05.014

Computer vision algorithm for barley kernel identification, orientation estimation and surface structure assessment

Piotr M. Szczypiński [1], Piotr Zapotoczny [2]

[1] Institute of Electronics, Technical University of Lodz, Wolczanska 211/215, 90-924 Lodz, Poland

[2] Department of Agri-Food Process Engineering, University of Warmia and Mazury in Olsztyn, Heweliusza 14, 10-718 Olsztyn, Poland

Abstract

This paper presents an algorithm for analyzing barley kernel images to evaluate cereal grain quality and perform grain classification. The input data comprised digital images of kernels obtained from an optical scanner. The algorithm identified individual kernels' smooth and wrinkled regions, described their orientation relative to the axis of symmetry, crease visibility and germ location. We were also able to determine the size of the wrinkled and smooth areas on a grain's surface, which allowed automatic grain classification and kernel quality assessment. The proposed algorithm was tested using barley grain images, and validated by comparison with the evaluation results of a professional assessor. The validation of the algorithm confirmed that it is efficient and robust allowing accurate description of over 93% of kernel samples in comparison with the expert.

Highlights

An algorithm to analyze barley kernel images was proposed.
The algorithm identified the wrinkled and smooth regions of individual kernels with a mean accuracy of 99%.
The algorithm eliminated the need for human involvement in the assessment process.

Keywords

Digital image analysis; Automated kernel grading; Cereal grain classification

1. Introduction

The process of manufacturing products of superior quality requires raw materials that are of equally high standard. The suitability of raw materials for industrial use is determined by their physical, chemical and sensory attributes. In plant breeding, the quality of seeds and parent material has a significant bearing on new varieties and breeding lines. Research centers around the world are attempting to develop quick and effective methods for evaluating the quality of raw materials, based on the assessment of selected attributes for specific applications in production and breeding (Brosnan and Sun, 2004, Mendoza et al., 2007 and Reum and Zhang, 2007).

The processing suitability of agricultural products is highly influenced by variable growing conditions and environmental factors. In the food processing industry, the quality grade of raw materials is classified (within the species) based on information about a given variety. This, however, has drawbacks. When affected by different environmental conditions, for example, the same genotype may produce different phenotypic responses (Jezowski, 1981 and Jezowski et al., 1993). Decisions on raw materials' processing suitability made solely on based on genotype features can be misleading (Rybinski and Szot, 2006). Several methods for analyzing grain varieties are available in practice, including immunological methods, DNA analyses, HPLC, protein electrophoresis and isoenzyme analyses (ISTA, 2012). Most of those techniques are expensive, time-consuming, and only available to specialist laboratories. Alternative methods for evaluating the quality and varietal uniformity of cereal grains are, therefore, needed. Computer image analyses, which offer such an alternative, have already been carried out for more than 10 years (Zayas and Steele, 1996, Neuman et al., 1987, Neuman et al., 1989a, Neuman et al., 1989b, Majumdar and Jayas, 1999, Majumdar and Jayas, 2000a, Majumdar and Jayas, 2000b, Majumdar and Jayas, 2000c and Majumdar and Jayas, 2000d). Jayas et al., 2000, Visen et al., 2001, Visen et al., 2002, Paliwal et al., 2001, Paliwal et al., 2003a and Paliwal et al., 2003b, and Zapotoczny et al. (2005). Shouche et al. (2001) used a flatbed scanner to discriminate fifteen Indian wheat varieties. From a group of 45 indices of geometric dimensions and shapes, they identified 5 indices that support varietal discrimination. Utku (2000) used a CCD camera to develop a system that distinguishes 31 wheat varieties. Various attempts have been made to identify grain classes and varieties based on differences in the geometric properties of kernels (Zayas et al., 1986, Shouche et al., 2001 and Brosnan and Da-Wen, 2002). Studies showed that vision systems (MVS) could successfully be used for identification of pests and the level of fungal infections in grains (Ruan et al., 2001 and Ridgway et al., 2002). MVS can also be used to analyze variations in the color of wheat grains caused by changes in moisture, fungal infections and overheating (Luo et al., 1999 and Ruan et al., 2001). Dalen (2004) used flatbed scanner images to evaluate the extent of damage to rice grains with 99% accuracy within a relatively short period of time (about 3 min). Strumiłło et al. (1999) developed a computer-aided system for evaluating the sowing suitability of seeds using X-ray images. In our previous study (Zapotoczny et al., 2008, Markowski et al., 2006, Zapotoczny, 2011a and Zapotoczny, 2011b), we relied on computer-assisted image analysis to discriminate between cereal grain varieties. Different varieties of wheat and malting barley grains were classified with an accuracy of nearly 100%. However our statistical models based on variables obtained from grains harvested in a given year failed to provide reliable results in successive years. Image analysis also proved to be an unsatisfactory method for evaluating grain quality (Zapotoczny, 2011a). The correlation coefficients between color, surface texture and geometric attributes of grains and the technological properties of the resulting flour were unsatisfactory (Zapotoczny, 2008). Previous studies focused on the evaluation of color, geometric and texture properties of individual kernels or bulk grain images. To our knowledge, there have been no attempts to measure the color, geometrical and textural features of parts of grain kernels such as dorsal (back) and ventral (front) sides of kernels, the crease and the germ. With regard to malting barley varieties, the wrinkled and the smooth sections of the kernel should be analyzed separately. The size and the attributes of the wrinkled surface are determined by varietal characteristics and the accumulation of reserve compounds in kernels. In this respect, this study attempted to develop an algorithm to automatically discriminate kernels positioned on the ventral or dorsal side and to identify various textured areas on the analyzed side. As a result, regions were identified, and color component (RGB, XYZ, L * ab), texture and shape descriptors of kernel surfaces were determined (Szczypinski et al., 2007 and Szczypinski et al., 2009). Our approach improved the efficiency of varietal discrimination by analyzing the correlations between variables obtained from the image analysis and the technological quality properties of grain (moisture content, germination energy, malting, total protein, viscosity, extraactivity of malt). The proposed system for evaluating the quality and varietal homogeneity of cereal grains could be dedicated to flour milling and grain processing companies.

This article proposes a computer-generated algorithm for preliminary analysis of kernel images. The algorithm will identify the imaged kernels, it will determine their orientation relative to their axis of symmetry, the location of the germ and the visibility of the crease (dorsal or ventral side of the kernel). The proposed algorithm will support image segmentation by identifying the areas of individual grains and the size of smooth and wrinkled areas on the grain's surface.

2. Materials and methods

2.1. Image analysis

Images of barley kernels (Fig. 1a) were obtained using an Epson 4490 flatbed scanner interfaced with a computer. The scanner uses a Charge Coupled Device (CCD) sensor array with the light sources located on its side, which allows to obtain fairly good focus on small three-dimensional objects such as kernels. The downside of this method of image acquisition is the uneven surface illumination of the kernels. Images were captured in color at a resolution of 400 DPI, 24 bits per pixel and stored in an uncompressed format not to introduce any additional artifacts. Kernels were positioned on the surface of the scanner in non-touching fashion, with a mean distance of at least 3 mm resulting in grain distance of at least 50% of the average grain's width, which allows to fit several hundred kernels in one image. For the acquisition the scanner's cover was removed and the scanner was placed in a compartment inlaid with black velvet. This resulted in images, in which the kernels are relatively bright compared with the dark background, allowing the application of simple and efficient computer algorithms to identify the kernel regions.

Kernels were placed by hand, they were roughly aligned with no predefined locations, thus their coordinates in the image are unspecified. Also, their orientations were not imposed, and thus some of them are visible from the dorsal side – the crease is not visible, whilst others show the ventral side exposing the crease. The kernel orientation with respect to the germ–brush direction (anteroposterior axis) was not predetermined, yet most of the kernels were aligned perpendicular to the scanner's image sensors array. Due to this fact and the already mentioned location of the light sources, the crease is noticeable as a darker line near the main axis of the kernels and the wrinkled region is visible as a texture comprising brighter and darker patches.

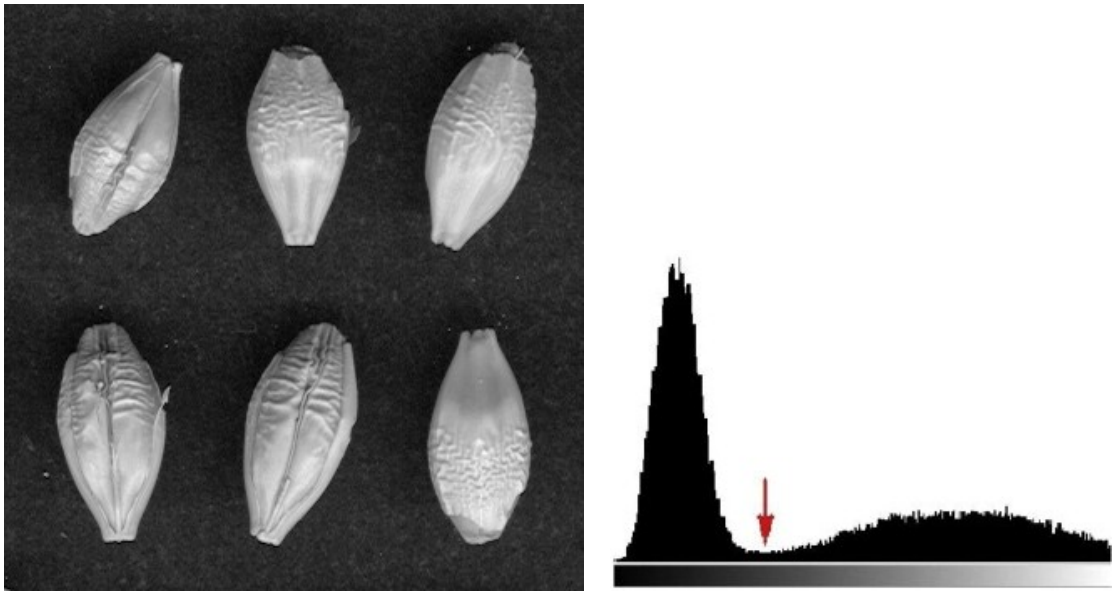

(a) (b)

Fig. 1. Example fragment of (a) the input image and (b) its histogram.

Based on the image properties we developed an image processing algorithm, which involves three key procedures. The first one is image segmentation and identification of individual kernels. The second one determines each kernel's orientation with respect to the dorsoventral and the anteroposterior axes. Finally, the third procedure aims at finding the wrinkled area of the kernel, since one of our goals is to verify whether the characteristics of the wrinkled region may be used for classification of varieties or assessing the dryness of kernels.

2.2. Segmentation and identification

The first step of the algorithm involves image segmentation or binarization (Gonzalez and Woods, 2006, Jähne and Haussecker, 2000 and Otsu, 1979), which splits the image pixels into two subsets: those that are a part of the background and those belonging to the kernel regions. The image histogram, which represents the number of pixels having the same brightness as a function of the brightness, is bimodal in the case of images under consideration (Fig. 1b). Therefore it shows two maxima, one related to the dark background and the other related to the brighter kernel regions, with a minimum in between. In this case the image segmentation is feasible by applying image grayscale thresholding – the pixels with a gray-level below that of the minimum fall into the background, while the rest are categorized as belonging to the kernels. In the binary image (Fig. 2a) positive values (white) represent the grain regions and zero values (black) represent the background. However, the contours of the kernels in the binary image are not always smooth. Moreover, the kernel areas are not always uniformly connected and some of them contain holes. What's more, there are some small crumb areas which may be incorrectly identified as kernels. To correct these discrepancies, we applied a procedure that involves the following three steps: (i) morphological opening with a circular structuring element of the radius equal to seven pixels; (ii) morphological closing with the same structuring element; and (iii) selection of regions based on their corresponding areas. The opening removes small-sized peninsula-shaped remains located near the kernel contours, while the closing removes any gulf-shaped cavities and open spaces. In addition, we estimated the mean area of the kernel regions in the images. Our procedure assumes that kernel areas should fall within the range of 50% and 150% of the mean. Following this assumption, regions with areas that are excessively small or excessively large are removed during the selection process (Fig. 2b), preventing the identification of small crumbs or multiple touching grains as individual kernels.

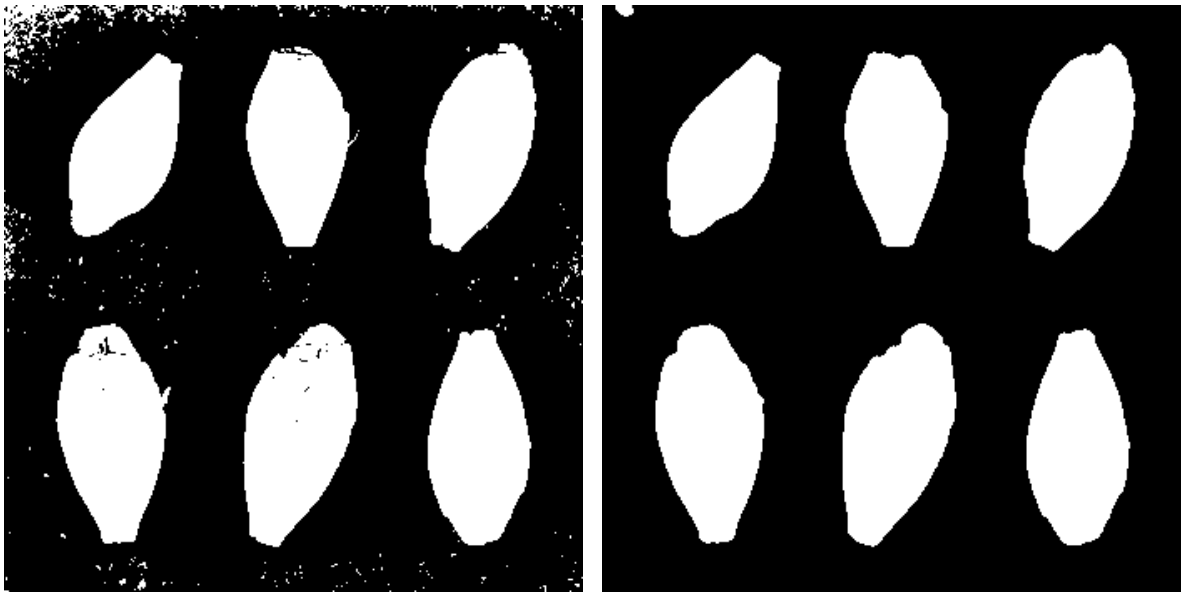

(a) (b)

Fig. 2. The result of the segmentation (a) after the image gray-scale thresholding and (b) followed by morphological closing and opening.

2.3. Orientation solving

As already mentioned, there are two aspects of orientation analysis, determination of orientation with respect to the anteroposterior and the dorsoventral axes. Therefore, our approach involves two steps of image analysis, the first one aims at localization of the longitudinal axis of symmetry and the second one establishes the presence of the crease.

To find the longitudinal axis of symmetry, which determines the germ–brush direction of each grain, all regions identified as kernels are analyzed one by one. In our approach, every region is approximated by an ellipse in such a way that the mean square distance between the region's contour and the ellipse is minimized (Hornberg, 2006 and Gander et al., 1994). It is assumed that every analyzed grain is quasi-symmetric and thus, the longer diameter of the ellipse aligns with the germ–brush line (Fig. 3). Since kernels are usually wider on the side of the germ and narrower on the other side, the average width of the region is measured independently on both sides of the kernel to determine the germ side. The sides are delimited by the shorter diameter of the ellipse and the width is measured in the direction parallel to that diameter. The higher value of the average width determines the germ side.

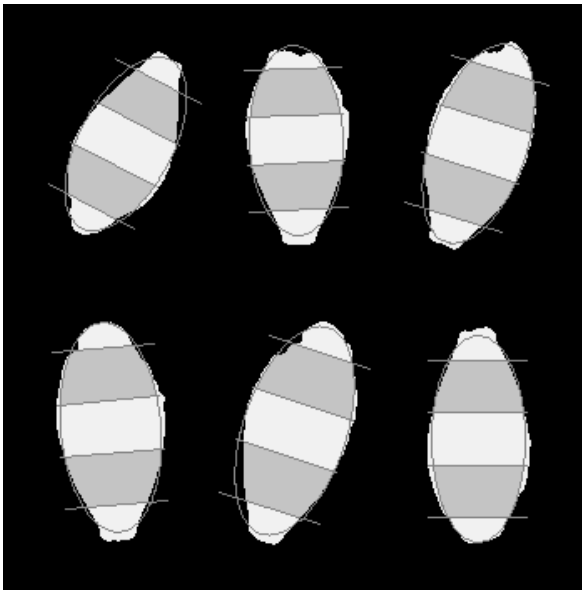

Fig. 3. Determination of grain germ–brush orientation.

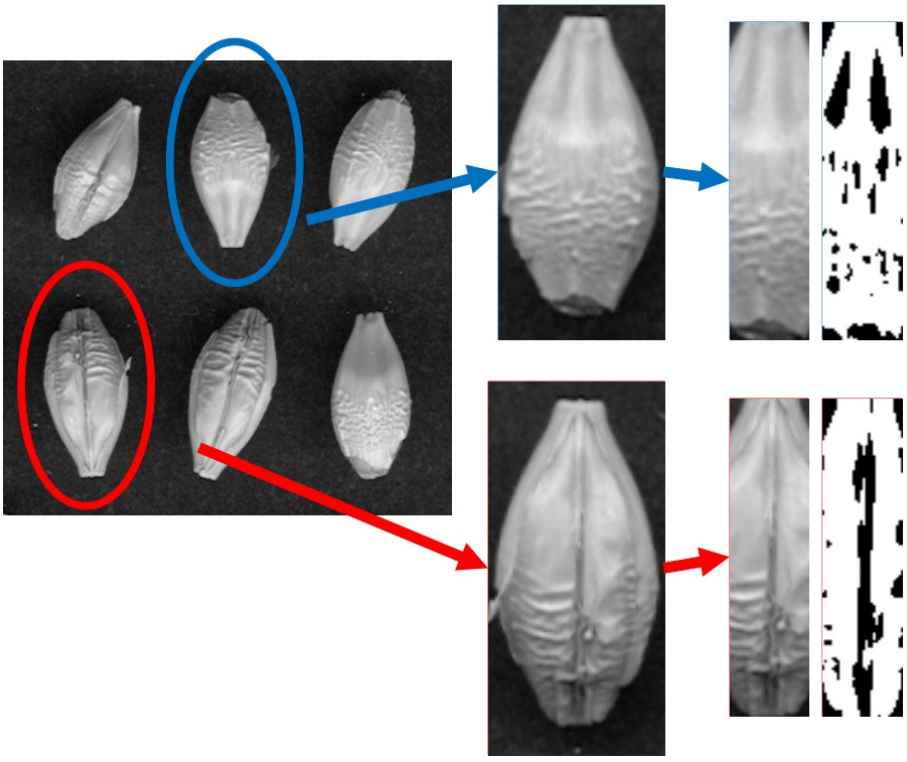

Fig. 4. Determination of the kernel's visible side: the dorsal (at the top row) and the ventral dorsal (at the bottom row).

At this stage, the kernels in the image are localized, their contours and areas are calculated, and the orientation of the germ–brush direction is known. In the next step every region, examined individually, is transformed onto a new image in such a way that the center of gravity of the grain becomes the center of the new image, the germ–brush direction is oriented vertically and the germ is positioned at the bottom. The new image size and transformation are computed based on the ellipse size and the orientation of its larger diameter. The transformed image's brightness function is interpolated by means of bilinear interpolation. The new image is used for the purpose of crease detection and later to find the wrinkled area.

The crease, if the ventral side of the kernel is visible, forms a dark elongated area stretching across the mid-line of the grain (Fig. 4). To determine the presence of that area we again use the image gray-level thresholding. In this case only the small rectangular area of the image is examined, the height of which is equal to the length of the larger diameter of the ellipse, the width equal to 1/4 of the ellipse width and its location being the central part of the kernel transformed image. We found that in most cases the crease of barley kernel resides in such a rectangular area and thus it is reasonable to limit the crease search to this region only. The threshold level used for the image segmentation is set individually for each kernel as the average gray-level within the rectangular area. After the segmentation, the lengths of any segments darker then the threshold value are measured. If any length is higher than half of the grain's length, the kernel is labeled as one with the ventral side visible. Otherwise, the kernel is labeled as visible from the dorsal side.

2.4. Wrinkled region detection

Wrinkled regions of the barley kernels are distinguished by a texture of brighter and darker patches. Therefore, to detect such regions automatically we use techniques of image texture analysis. Textures are defined as visualizations of repeated patterns that are perceived by humans as uniform and homogeneous in appearance. Despite those perceptions, textures are usually not uniform in terms of image gray-levels. Therefore, segmentation of textured images, performed to determine texture diversity, is not feasible with gray-level thresholding. To overcome this problem, texture descriptors (features) are usually computed. Descriptors are numerical values which quantitatively characterize specific texture properties, such as roughness, directivity, randomness, smoothness or granulation. If two textures differ with respect to a given descriptor, that descriptor can be applied in texture discrimination and for image segmentation. In our approach, the descriptor was computed at every image location and its value was thresholded to segment the image into areas corresponding to different textures. Finding a particular feature capable to reliably discriminate the textures of interest (the wrinkled and smooth regions of kernels) was one of goals of our study.

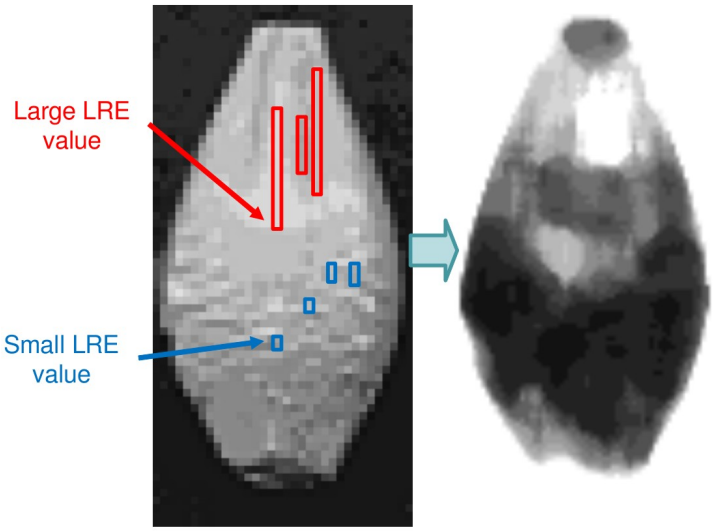

Fig. 5. Mapping the LRE moments.

To accomplish this task the MaZda software (Szczypinski et al., 2007, Szczypinski et al., 2009, Szczypiński et al., 2011, Klepaczko et al., 2010 and Thybo et al., 2004) was applied to find the texture descriptor capable of correct discrimination of the two areas. The software can compute up to several hundred various texture descriptors and then it estimates their discriminative strength. We found the Long Runs Emphasis (LRE) (Haralick, 2005) moment of the run-length matrix (RLM) computed for vertical runs proved to be most effective in differentiating the areas of interest. The RLM holds counts of pixel runs with the specified gray-scale level and length (Fig. 5). It can be computed for a chosen direction of pixel runs, such as horizontal or vertical. The LRE moment's value is higher if many long runs of pixels have similar gray-levels. Otherwise its value is low. Smooth areas of homogeneous brightness level result in long runs and a high corresponding LRE value. On the other hand, wrinkled areas are characterized by low LRE values.

Based on RLM's LRE moment, an algorithm that facilitates wrinkled area extraction was developed. The algorithm takes the rotated image of an individual kernel as the input. For every pixel of the input image, pixels in the vertical run including that pixel and having a similar gray-scale to the pixel, are counted. The brightness of all the pixels in a run may vary from the brightness of the reference pixel by no more than k, where k is a parameter of the algorithm. Next, the corresponding pixel in the output image is substituted with the number of counted pixels in the run. Following this, the output image is smoothed by means of a median $n \times n$ filter, and thresholded at the level of t, where n and t are also parameters of the algorithm. The experiment was performed to establish appropriate values of the algorithm parameters. The reference image was used, in which an experienced assessor depicted the wrinkled regions manually. It was established that wrinkled regions automatically detected are comparable with regions manually outlined for $k = 8$, $n = 3$ and $t = 5$. Thus, this set of parameters was used for analysis of other images of barley kernels.

3. Results and discussion

3.1. Algorithm validation

The algorithm was written in C language and compiled for the *Microsoft Windows* platforms utilizing the Intel's OpenCV library implementations of basic image processing operations. The computation time was measured on a 2673 × 4031 pixels color image of 543 Blask barley kernels – 272 on dorsal sides and 271 on ventral sides. On a computer with a 650 GHz Intel i5 CPU the algorithm took 68 s to process the image (126 ms per kernel). The algorithm correctly identified and counted all the kernels in the image, it correctly identified the germ–brush direction in 532 cases (98%) and dorsoventral orientation in 525 cases (96.7%). Selected kernels which produced incorrect results are presented in Fig. 6. In Fig. 6a, the crease was not exposed, but the presence of a black line of elongated fold casing led to incorrect classification. Fig. 6b shows a highly asymmetric kernel whose orientation was incorrectly recognized due to a side-wise location of the crease. The grain in Fig. 6c is abnormally narrow on the germ side, and as the result, the germ–brush direction was incorrectly identified.

The algorithm was developed to support image segmentation and specify the regions corresponding to individual grains and sub-regions of wrinkled areas. To validate the segmentation procedure, the regions produced by the algorithm were compared with the corresponding regions depicted by a professional grain quality assessor. The number of pixels was counted, including pixels belonging to both regions (number of true positives – TP), pixels belonging only to the manually depicted region (number of false negatives – FN) and pixels belonging exclusively to the automatically obtained region (number of false positives – FP). Subsequently, three quantitative measures were computed: the Jaccard similarity coefficient (ratio of TP to the sum of TP, FN and FP), precision (ratio of TP to the sum of TP and FP) and recall (ratio of TP to the sum of TP and FN). The average values of quantitative measures, averaged for all grains, and standard deviation values are listed in Table 1 and Table 2. Selected examples of the compared regions are presented in Fig. 7.

(a) (b) (c)

Fig. 6. Selected kernels with incorrectly determined orientations: (a) grain with an elongated fold incorrectly recognized as crease, (b) deformed, asymmetric grain whose crease was not detected, and (c) grain with incorrectly identified germ–brush direction.

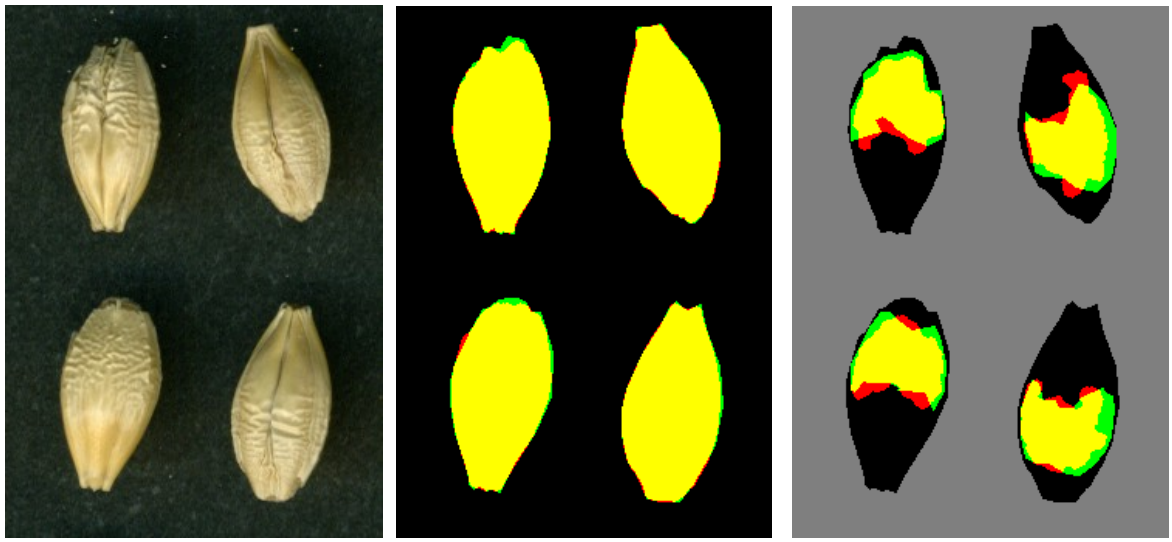

(a) (b) (c)

Fig.7. A comparison of manually and automatically depicted regions: (a) original image, (b) regions corresponding to individual grains, and (c) regions of wrinkled areas. The regions depicted by the assessor are marked green (FN area), the regions depicted automatically are shown in red (FP area), and the intersection of two regions (TP area) is marked yellow.

The further validation of the algorithm involved analysis of 11 varieties of barley kernels at three different levels of moisture content – altogether 33 images showing over 15,800 kernels. The results obtained by automatic image analysis were than verified by an experienced assessor, who pointed out and counted improperly recognized kernels. The assessment considered the indication of the kernel and wrinkled area regions, as well as the determination of dorsoventral and germ–brush orientations. The summary of the results obtained automatically and the results of the assessment are presented in Table 3. It shows the number of kernels per image ranged from 476 up to 480. The number of omitted or unidentified kernels per image ranged from zero up to four, which amounted in 0.1% of the total number of kernels. In all such cases the error was caused by failure to keep adequate distances between kernels. There were 77 cases (0.49%) of kernels for which the wrinkled area was incorrectly outlined, ranging from zero up to seven cases per image. The dorsoventral orientation was incorrectly recognized in 4.12% of all kernels. It must be noted that the largest number of such errors occurred in the Prymus variety, for which the dissimilarity of a kernel's width at the germ and the brush sides are not as evident as in the other varieties. Finally, the brush–germ orientation was incorrectly determined in 1.61% of all kernels – in most

such cases the kernels were deformed, their shape was distorted or a fragment was missing. Total percentage of correctly recognized and depicted kernels reached 93.7%.

4. Conclusions

In this study, we presented a novel algorithm for analyzing visual images of barley kernels. The algorithm identified and counted kernels within the image, depicted wrinkled and smooth regions of kernels and also determined orientation relative to the germ–brush direction and the location of the crease. The validation of the algorithm confirmed that it is efficient and robust allowing accurate description of over 93% of kernel samples. The regions of individual kernels determined automatically matched the areas identified by the expert with a high degree of precision.

Further studies are planned to identify the correlations between texture and color parameters of the studied regions and the technological properties of grain. The algorithm is planned to be used in the preprocessing of hyperspectral images, which significantly expands its scope of application. We expect that the proper identification of kernel regions and their orientations will enable more accurate recognition of the grain varieties, moisture estimation or potential for germination and growth. Moreover, the proposed algorithm eliminates the need for human involvement in the assessment process, thus increasing the objectivity, reliability and reproducibility of the results generated by the automated procedure.

Acknowledgment

The author are grateful for the financial support provided by the Ministry of Scientific Research within the framework of Grant No. 4498/B/P01/2010/39.

References

Brosnan, T., Da-Wen, Sun. 2002. Inspection and grading of agricultural and food products by computer vision systems – a review. Comput. Electron. Agric., 36:193-213.

Brosnan, T., Sun, D.W. 2004. Improving quality inspection of food products by computer vision – a review. Journal of Food Engineering, 61, 3–16.

Dalen, G. 2004. Determination of size distribution and percentage of broken kernels of rice using flatbed scaninig and image analysis. Food Research International. 37, 51-58

Gander, W., Golub, G.H., Strebel, R., 1994. Fitting of Circles and Ellipses, Least Square Solution. Tech. Rep. 1994TR-217. ETH Zurich, Institute of Scientific Computing.

Gonzalez R.C., Woods R.E. 2006, Digital Image Processing, Prentice-Hall, Inc., Upper Saddle River, NJ (2006)

Haralick, R. M., “Statistical and structural approaches to texture,” Proceedings of the IEEE, vol. 67, no. 5, pp

Homberg A. 2006, Handbook of Machine Vision, Wiley-VCH, John Wiley, Weinheim, Chichester (2006)

International Rules for Seed Testing. 2011. International Seed Testing Associations ISTA, Edition 2011part 8.8 www.seedtest.org

Jähne B. and Haussecker H., 2000, Computer Vision and Applications: A Guide for Students and Practitioners, Academic Press, San Diego (2000)

Jayas, D.S., Paliwal, J., Visen, N.S. 2000. Multi-layer neural networks for image analysis of agricultural products. J. Agric. Engang. Res. 77(2), 119-128

Jezowski S., Surma M., and Adamski T., 1993. Genetic parameters for some morphological and physiological characteristics of the stem of barleyDHlines (in Polish). Zesz. Nauk. AR Wroclaw, 223, 215-221.

Jezowski, S., 1981. Analysis of relationship between lodging grade and some morphological characteristics determining lodging resistance of barley. Genet. Pol., 28: 33-38.

Klepaczko, A., Szczypiński, P., Daniel, P., Pazurek, M. 2010. Local Polynomial Approximation for Unsupervised Segmentation of Endoscopic Images”, in Computer Vision and Graphics, t. 6375, Red. Berlin, Heidelberg: Springer Berlin Heidelberg, s. 33-40.

Luo, X., Jayas, D.S., Symons, S.J. 1999. Identifications of damaged kernels in wheat using a colour machine vision system. Journal of Cereal Science. 30, 49-59

Majumdar, S., Jayas, D.S. 2000a. Classification of cereal grains using machine vision: I. Morphology models. American Society of Agricultural Engineering. 43(6) 1669-1675

Majumdar, S., Jayas, D.S. 2000b. Classification of cereal grains using machine vision: III. Texture Models. Morphology

models. American Society of Agricultural Engineering. 43(6) 1681-1687
Majumdar, S., Jayas, D.S. 2000c. Classification of cereal grains using machine vision: II. Color Models. Morphology models. American Society of Agricultural Engineering. 43(6) 1677-1680
Majumdar, S., Jayas, D.S. 2000d. Classification of cereal grains using machine vision: VI. Combined Morphology, Color, and Texture Models. American Society of Agricultural Engineering. 43(6) 1689-1694
Markowski M., Ratajski A., Konopko H., Zapotoczny P., Majewska K. 2006, Rheological behavior of hot-air-puffed amaranth seeds, Int. J. Food Propert., 9 (2), pp. 195–203.
Mendoza, F, Dejmek, P., Agullera, J.M. 2007. Colour and image texture analysis in classification of commercial of commercial potato chips. Food Research International, 40(9), 1146-1154.
Neuman, M., Sapristein, H D., Shwedyk, E., Bushuk, W. 1987. Discrimination of wheat class and variety by digital image analysis of whole grain samples. Journal of Cereal Science. 6, 125-132
Neuman, M., Sapristein, H D., Shwedyk, E., Bushuk, W. 1989a. Wheat grain color analysis by digital image processing: I. Methodology. Journal of Cereal Science. 10(3), 175-182
Neuman, M., Sapristein, H D., Shwedyk, E., Bushuk, W. 1989b. Wheat grain color analysis by digital image processing: II. Wheat class determination. Journal of Cereal Science. 10(3), 183-182
Otsu, N. 1979. A threshold selection method from gray-level histograms, systems, man and cybernetics, IEEE Trans., 9 (1) (1979), pp. 62–66
Paliwal, J., Visen, N.S., Jayas, D.S. 2001. Evaluation of neural network architectures for cereal classification using morphological features. J. Agric. Engang. Res. 79(4), 361-370.
Paliwal, J., Visen, N.S., Jayas, D.S., White N.D.G. 2003a. Cereal grain and dockage identification using machine vision. Biosystems Engineering. 85(1), 51-57
Paliwal, J., Visen, N.S., Jayas, D.S., White N.D.G. 2003b. Comparison of a neural network and non-parametric classifier for grain kernel identification. Biosystems Engineering. 85(4), 405-413
Reum, D., Zhang, Q. 2007. Wavelet based multi-spectral image analysis of maize leaf chlorophyll content Original Research Article, Computers and Electronics in Agriculture, 56, (1), 60-71.
Ridgway, C., Davies, E.R., Chambers, J., Mason, D.R., Bateman, M. 2002. Rapid machine vision method for the detection of insects and other particulate bio-contaminants of bulk grain in transit. Biosystems Eng., 83 (1): 21-30.
Ruan, R., Ning, S., Luo, L., Chen, X., Chen, P., Jones, R., Wilcke, W., Morey, V. 2001. Estimation of weight percentage of scabby wheat kernels using an automatic machine vision and neural network based system. Trans. ASAE, 44 (4): 983-988.
Rybiński, W., Szot, B. 2006. Estimation of genetic variability of yielding traits and physical properties of seeds of spring barley (Hordeum vulgare L.) mutants. Int. Agrophysics, 20:, 219-227.
Shouche, S.P., Rastogi, R., Bhagwat, S.G., Sainis, J.K. 2001. Shape analysis of grains of Indiana wheat varieties. Computers and electronics in agriculture. 33, 55-76
Strumiłło, P., J. Niewczas, P. Szczypiński, P. Makowski, and W. Woźniak, 1999. Computer System for Analysis of X-Ray Images of Wheat Grains, Int. Agrophysics, vol. 13, no. 1, pp. 133-140.
Szczypinski, P. M, Strzelecki, M., Materka, A. 2007. Mazda - a software for texture analysis, International Symposium on Information Technology Convergence (ISITC 2007), Jeonju, Korea, 2007, pp. 245-249.
Szczypinski, P. M, Strzelecki, M., Materka, A., Klepaczko, A. 2009. MaZda - A software package for image texture analysis," Computer Methods and Programs in Biomedicine, vol. 94, no. 1, pp. 66-76.
Szczypiński, P., Klepaczko, A., Strzelecki, M. 2011. An Intelligent Automated Recognition System of Abnormal Structures in WCE Images", in Hybrid Artificial Intelligent Systems, t. 6678, E. Corchado, Berlin, Heidelberg: Springer Berlin Heidelberg, s. 140-147.
Thybo, A. K., Szczypinski, P. M, Karlsson, A. H, Donstrup, S. Stodkilde-Jorgensen H. S, and. Andersen H. J, 2004, Prediction of sensory texture quality attributes of cooked potatoes by NMR-imaging (MRI) of raw potatoes in combination with different image analysis methods, Journal of Food Engineering, vol. 61, no. 1, pp. 91-100.
Utku, H. 2000. Application of the feature selection method to discriminate digitized wheat varieties. Journal of Food Engineering. 46, 211-216
Visen, N.S., Paliwal, J., Jayas, D.S., White, N.D.G. 2001. Specialist neural networks for cereal grain classification. Biosystems Engineering. 82(2), 151-159
Visen, N.S., Shashidhar, N.S., Paliwal, J., Jayas, D.S. 2002. Identification and segmentation of occluding groups of grain kernels in a grain sample image. J. Agric. Engang. Res. 79(2), 159-166
Zapotoczny P. 2008. The method of assessing the quality of wheat using computer vision systems for obtaining a unification of the material. National Science Centre. 1089/P06/2005/29 (in. polish)
Zapotoczny, P. 2011a. Discrimination of Wheat Grain Varieties Using Image Analysis and Neural Networks. Part I. Single kernel texture. Journal of Cereal Science, 54 (1); 60-68
Zapotoczny, P. 2011b. Discrimination of wheat grain varieties using image analysis: morphological features. European Food Research and Technology. 233, 769–779
Zapotoczny, P. Zielińska, M. Nita, Z. 2008. Application of image analysis for the varietal classification of barley. morphological features. Journal of Cereal Science 48 (2008) 104–110
Zapotoczny, P., Majewska, K. 2010. A comparative analysis of color measurements of the seed coat and endosperm of wheat kernels performed by various techniques. International Journal of Food Properties, 13: 1–15.

Zayas, I.Y., Lai F.S., Pomeranz Y. 1986. Discrimination between wheat classes and varieties by image analysis. Cereal Chem., 63 (1): 52-56.
Zayas, I.Y., Steele, J.L. 1996. Image texture analysis for discrimination of mill fractions of hard and soft wheat. Cereal Chem., 73 (1): 136-142.
OpenCV 2.1 C++ Reference — opencv v2.1 documentation.” [Online]. Available: http://opencv.willowgarage.com/documentation/cpp/index.html. [Accessed: 03-Nov-2011].

Table 1. Quantitative measures of similarity between kernel regions.

Similarity indices	Average	Standard deviation
Jaccard coefficient	0.966	0.009
Sensitivity	0.974	0.010
Precision	0.991	0.004

Table 2. Quantitative measures of similarity between wrinkled regions.

Similarity indices	Average	Standard deviation
Jaccard coefficient	0.712	0.068
Sensitivity	0.811	0.078
Precision	0.858	0.068

Table 3. Assessment of the automatic analysis results on various varieties of barley kernels.

Variety	Moisture content (%)	Detected kernels	Omitted kernels	Incorrect wrinkled region	Incorrect brush–germ orientation	Dorsal side detected	Ventral side incorrectly detected	Ventral side detected	Dorsal side incorrectly detected
Prymus	12	479	0	1	35	196	7	283	47
	14	480	0	7	31	182	3	298	37
	16	479	0	4	37	188	9	291	38
Serwal	12	479	0	5	4	214	15	265	11
	14	480	0	3	4	231	8	249	12

	16	479	0	0	7	221	15	258	10
Signora	12	479	0	0	3	257	6	222	6
	14	478	2	3	2	253	8	225	8
	16	479	0	0	1	273	5	206	4
STH	12	479	0	2	1	185	3	294	23
	14	479	0	2		218	13	261	31
	16	479	0	1	1	187	6	292	18
Victorina	12	479	0	1	1	261	10	218	1
	14	478	0	2	5	228	6	250	1
	16	476	0	1	4	232	7	244	2
Afrodita	12	476	2	4	3	223	2	253	13
	14	480	0	3	5	209	1	271	8
	16	478	2	4	6	204	1	274	16
Blask	12	479	0	1	3	231	10	248	3
	14	478	0	3	7	229	10	249	4
	16	478	2	2	9	235	12	243	1
Bordo	12	480	0	2	4	266	12	214	1
	14	480	0	2	6	253	9	227	3
	16	479	0	5	3	256	8	223	2
Conchita	12	478	2	4	6	208	5	270	11
	14	479	0	2	4	224	5	255	5
	16	476	2	3	7	226	9	250	11
Kormoran	12	478	0	4	6	226	2	252	6
	14	478	0	1	11	228	5	250	9
	16	479	0	2	10	190	3	289	13
Mercanda	12	475	4	1	12	218	11	257	15
	14	478	0	0	3	254	12	224	14
	16	479	0	2	13	228	11	251	17
Total error (%)	–	–	0.10	0.49	1.61	–	1.58	–	2.54